Ince–Gaussian modes of the paraxial wave equation and stable resonators

Miguel A. Bandres and Julio C. Gutiérrez-Vega

Photonics and Mathematical Optics Group, Tecnológico de Monterrey, Monterrey, México, 64849

Received August 18, 2003; revised manuscript received December 5, 2003; accepted December 10, 2003

We present the Ince–Gaussian modes that constitute the third complete family of exact and orthogonal solutions of the paraxial wave equation in elliptic coordinates and that are transverse eigenmodes of stable resonators. The transverse shape of these modes is described by the Ince polynomials and is structurally stable under propagation. Ince–Gaussian modes constitute the exact and continuous transition modes between Laguerre– and Hermite–Gaussian modes. The expansions between the three families are derived and discussed. As with Laguerre–Gaussian modes, it is possible to construct helical Ince–Gaussian modes that exhibit rotating phase features whose intensity pattern is formed by elliptic rings and whose phase rotates elliptically. © 2004 Optical Society of America

OCIS codes: 260.1960, 350.5500, 140.3300, 050.1960, 140.3410.

1. INTRODUCTION

Hermite–Gaussian modes (HGMs) and Laguerre–Gaussian modes (LGMs) exhibit three important properties: They form two complete families of exact and orthogonal solutions of the paraxial wave equation (PWE), they are transverse eigenmodes of stable resonators, and they do not change shape on propagation, i.e., they are structurally stable.[1] HGMs have a rectangular geometry that is inherent in Cartesian coordinates, whereas LGMs are rotationally symmetric and exhibit an azimuthal angular dependence of the real form $\cos(l\phi)$, $\sin(l\phi)$, or of the complex form $\exp(\pm il\phi)$. The properties and applications of these families have been widely studied for more than 40 years.[2] Recent research has concerned the conversion between HGMs and LGMs in relation to the transfer of angular momentum[3] and meaningful similarities between these modes and the eigenstates of the two-dimensional quantum harmonic oscillator.[4]

In the present paper we introduce the Ince–Gaussian modes (IGMs), which form a third family of exact and orthogonal solutions of the PWE in elliptic coordinates, are natural resonating modes in stable resonators, and constitute the exact and continuous transition modes between HGMs and LGMs. The transverse distribution of these fields is described by the Ince polynomials,[5–7] and (like HGMs and LGMs) constitute a complete set of solutions of the PWE, such that any paraxial field can be expressed as a superposition of IGMs. The propagating and resonating characteristics of the IGMs are discussed and compared with the corresponding ones of HGMs and LGMs. We have found that IGMs tend to LGMs or HGMs as the ellipticity parameter tends to zero or infinity, respectively. The expansions of IGMs in terms of LGMs and HGMs and vice versa are derived and their mathematical properties discussed. IGMs describe satisfactorily natural resonating modes within stable resonators, and with them a novel class of rotating waves with elliptic helical structure can be constructed.

2. INCE–GAUSSIAN MODES

To derive the IGM we proceed as follows: For a paraxial field traveling in the z direction we write $U = \Psi(\xi, \eta, z)\exp(ikz)$, where (ξ, η) are the transverse coordinates and Ψ is a slowly varying complex envelope that satisfies the PWE,

$$\left(\nabla_t^2 + 2ik\frac{\partial}{\partial z}\right)\Psi(\mathbf{r}) = 0, \tag{1}$$

where ∇_t^2 is the transverse Laplacian, $\mathbf{r}$ is the position vector, and k is the wave number. The lowest-order solution of the PWE is the fundamental Gaussian beam (GB),

$$\Psi_G(\mathbf{r}) = \frac{w_0}{w(z)}\exp\left[\frac{-r^2}{w^2(z)} + i\frac{kr^2}{2R(z)} - i\psi_{\mathrm{GS}}(z)\right], \tag{2}$$

where r is the radius, $w^2(z) = w_0^2(1 + z^2/z_R^2)$ describes the beam width, $R(z) = z + z_R^2/z$ is the radius of curvature of the phase front, $\psi_{\mathrm{GS}}(z) = \arctan(z/z_R)$ is the Gouy shift, $z_R = kw_0^2/2$ is the Rayleigh range, and w_0 is the beam width at $z = 0$.

To obtain solutions of the PWE in elliptical coordinates we will consider a wave whose complex envelope is a modulated version of the GB,

$$\mathrm{IG}(\mathbf{r}) = E(\xi)N(\eta)\exp[iZ(z)]\Psi_G(\mathbf{r}), \tag{3}$$

where E, N, and Z are real functions.

In a transverse z plane, we define the elliptic coordinates as $x = f(z)\cosh\xi\cos\eta$, $y = f(z)\sinh\xi\sin\eta$, and $z = z$, where $\xi \in [0,\infty)$ and $\eta \in [0,2\pi)$ are the radial and the angular elliptic variables, respectively.[8] Curves of constant ξ are confocal ellipses, and curves of constant η are confocal hyperbolas. The semifocal separation f diverges in the same way as the width of the GB, i.e., $f(z) = f_0 w(z)/w_0$, where f_0 is the semifocal separation at the waist plane $z = 0$.

The field IG ($\mathbf{r}$) has two important physical properties: First, the phase is the same as that of the underlying GB, except for an excess phase $Z(z)$. If Z is a slowly varying function of z (as required by the paraxial approximation), the waves IG and Ψ_G have paraboloidal wave fronts with the same radius of curvature $R(z)$; thus they are focused by lenses and mirrors in precisely the same way. Second, the magnitude of IG ($\mathbf{r}$) varies with z in accordance with the same scaling factor $1/w(z)$ as GBs. The IGM therefore represents a beam of non-Gaussian intensity distribution, but with the same wave fronts and angular divergence as the GB.

The existence of the IGM is ensured if three real functions $E(\xi)$, $N(\eta)$, and $Z(z)$ can be found such that Eq. (3) satisfies the PWE in elliptical coordinates. Inserting the trial solution into the PWE and using the fact that $\Psi_G(\mathbf{r})$ itself satisfies the PWE, we obtain the three ordinary differential equations

$$\frac{\mathrm{d}^2E}{\mathrm{d}\xi^2} - \epsilon \sinh 2\xi \frac{\mathrm{d}E}{\mathrm{d}\xi} - (a - p\epsilon \cosh 2\xi)E = 0, \quad (4)$$

$$\frac{\mathrm{d}^2N}{\mathrm{d}\eta^2} + \epsilon \sin 2\eta \frac{\mathrm{d}N}{\mathrm{d}\eta} + (a - p\epsilon \cos 2\eta)N = 0, \quad (5)$$

$$-\left(\frac{z^2 + z_R^2}{z_R}\right)\frac{\mathrm{d}Z}{\mathrm{d}z} = p, \quad (6)$$

where p and a are separation constants, and $\epsilon = 2f_0^2/w_0^2$ is the ellipticity parameter. From Eq. (6) the excess phase is given by $Z(z) = -p \arctan(z/z_R)$.

Equation (5) is known in the theory of periodic differential equations under the name Ince equation; it was studied originally by the mathematician E. G. Ince in 1923.[5] The Ince equation is a special case of the most general Hill equation and it has been investigated in detail by F. M. Arscott[6,7]; it is his notation for the solutions that we use. Note that Eq. (4) may be derived from Eq. (5) by writing $i\xi$ for η, and vice versa. This reciprocal relation is important because radial solutions $E(\xi)$ may be obtained from angular solutions $N(\eta)$ by making the argument imaginary. There are three parameters in Eq. (5); it is convenient to regard ϵ as fundamental and a, p as disposable parameters. The technique for solving Eq. (5) analytically is very similar to that for the better known Mathieu equation.[8] Qualitatively, Eq. (5) differs from the Mathieu equation in that for certain values of a and p, there exist finite solutions, i.e., solutions expressible as finite trigonometric series or as polynomials in $\sin\eta$ or $\cos\eta$. In Appendix A we review the basic theory and properties of the Ince equation and its solutions.

Solutions of Eq. (5) are known as the even and odd Ince polynomials of order p and degree m; they are usually denoted as $C_p^m(\eta, \epsilon)$ and $S_p^m(\eta, \epsilon)$, respectively, where $0 \leqslant m \leqslant p$ for even functions, $1 \leqslant m \leqslant p$ for odd functions, the indices (p, m) always have the same parity, i.e. $(-1)^{p-m} = 1$, and ϵ is the ellipticity parameter defined earlier.[6]

Expression (3) corresponds then to the mathematical description of the IGM, if one inserts the product of Ince polynomials on the right-hand side. If we look for three-dimensional solutions, only products of functions of the same parity in ξ and η satisfy the continuity in the whole space; thus rearranging terms and multiplying by $\exp(ikz)$ provides the general expressions of the even and odd IGMs,

$$\mathrm{IG}_{p,m}^{e}(\mathbf{r}, \epsilon) = \frac{\mathcal{C}w_0}{w(z)} C_p^m(i\xi, \epsilon) C_p^m(\eta, \epsilon) \exp\left[\frac{-r^2}{w^2(z)}\right] \times \exp i\left[kz + \frac{kr^2}{2R(z)} - (p+1)\psi_{\mathrm{GS}}(z)\right], \quad (7)$$

$$\mathrm{IG}_{p,m}^{o}(\mathbf{r}, \epsilon) = \frac{\mathcal{S}w_0}{w(z)} S_p^m(i\xi, \epsilon) S_p^m(\eta, \epsilon) \exp\left[\frac{-r^2}{w^2(z)}\right] \times \exp i\left[kz + \frac{kr^2}{2R(z)} - (p+1)\psi_{\mathrm{GS}}(z)\right], \quad (8)$$

where $\mathcal{C}$ and $\mathcal{S}$ are normalization constants and the superindices e and o refer to even and odd modes, respectively. Since $C_0^0(\eta, \epsilon) = 1$, the IGM with indices (0, 0) is simply the lowest-order GB.

3. PROPAGATING AND RESONATING CHARACTERISTICS

To fully describe the transverse distribution of an IGM at the waist plane, we need to give the parity, the indices p and m, and two of the three following parameters: ϵ, w_0, and f_0, where $\epsilon = 2f_0^2/w_0^2$. The physical meaning of these last quantities is important; whereas the dimensionless parameter ϵ adjusts the ellipticity of the transverse structure of the beam, the parameters w_0 and f_0 scale the physical size of the mode.

Several transverse shapes of even and odd low-order IGMs at the waist plane $z = 0$ are shown in Fig. 1. As we know of no available numerical routines to compute the Ince polynomials, we developed our own algorithms to compute them based on their theory (see Appendix A). The phase of the higher-order modes exhibits clearly the elliptical structure of the IGMs. Note that m corresponds to the number of hyperbolic nodal lines, whereas $(p - m)/2$ is the number of elliptic nodal lines, without taking into account the interfocal nodal line at $\xi = 0$ for the odd modes. Beams of higher indices have a larger extent than those of lower indices.

Most of the propagating and resonating characteristics of the HGMs and LGMs can be extended straightforwardly to the IGMs. For instance, regardless of the indices, the width of the beam is proportional to $w(z)$, so that as z increases, the transverse intensity pattern is affected by the factor $w_0/w(z)$ but otherwise is shape invariant. This result follows from the fact that the transverse shapes exist in an elliptic coordinate system whose foci evolve according to $f(z) = f_0 w(z)/w_0$ as the beam propagates; therefore the eccentricity of the elliptic and hyperbolic nodal lines is invariant under propagation. The radius of curvature $R(z)$ in Eq. (2) is the same for all

IGMs, implying that the IGMs have the same wave fronts and angular divergence as the GBs.

IGMs at any z plane are orthonormal with respect to the indices and the parity; thus we have

$$\int \int_{-\infty}^{\infty} \mathrm{IG}_{p,m}^{\sigma} \overline{\mathrm{IG}}_{p',m'}^{\sigma'} \mathrm{d}S = \delta_{\sigma\sigma'} \delta_{pp'} \delta_{mm'}, \tag{9}$$

where the overbar denotes the complex conjugate, δ is the Kronecker delta function, dS is the differential surface element, and $\sigma = \{e,o\}$ is the parity.

The Gouy phase shift is a function of the order; for IGM we obtain $\psi_{\mathrm{IG}}(z) = (p + 1)\psi_{\mathrm{GS}}(z)$. This means that the phase velocity increases with increasing order number. In resonators this leads to differences in the resonance frequencies of the various IGMs of oscillation; that is, for a two-mirror cavity of length L we obtain

$$\omega_{sp} = \frac{c}{L}[s\pi + (p + 1)\cos^{-1}(\pm\sqrt{g_1 g_2})], \tag{10}$$

where s is the number of half-wavelengths along the axis of the resonator, c is the light velocity, and $g_j = 1 - L/R_j$ are the g parameters of the resonator.[1] As with GB, the complex beam parameter $q(z)$ of the beam is sufficient for propagating an IGM through a paraxial optical system characterized by an *ABCD* matrix by means of the well-known bilinear equation[1]

$$q_{\mathrm{out}} = \frac{Aq_{\mathrm{in}} + B}{Cq_{\mathrm{in}} + D}. \tag{11}$$

In order to corroborate the properties of the IGM discussed above, we have implemented the classical Fox–Li method to determine numerically the passive three-dimensional field structure of an IGM within a stable two-mirror cavity.[9] For this purpose, the diffractive field calculations are based on the angular spectrum of the plane waves representation by using the two-dimensional fast Fourier transform algorithm. The transverse field is sampled over a grid of 512×512 points. The three-dimensional intracavity field distribution is obtained by calculating the field at 200 transverse planes evenly spaced through the unfolded cavity. MATLAB software was used to implement the codes, mainly because of its inclusion of a wealth of built-in mathematical functions.

For numerical purposes we chose wavelength $\lambda = 632.8$ nm (typical of He–Ne lasers) and cavity length $L = 1$ m. To show clearly the waist and divergence of the beam, the curvature radii of the mirrors were chosen as $R_1 = 2$ m and $R_2 = 1.6$ m. To induce the Ince–Gaussian distribution, we started our simulation at mirror 1 using as initial condition the field $\mathrm{IG}_{6,2}^{e}(\xi, \eta, \epsilon = 2)$ depicted in Fig. 1, properly modulated by a spherical phase factor. The intracavity field distribution along the planes *x,z* and *y,z* is presented in Fig. 2. For the input data, the waist is located theoretically at 0.375 m from the mirror 1, and the spot size is given by $\omega_0 = 0.4$ mm. Figure 2 clearly illustrates the Gaussian evolution of the IGM within the cavity.

We performed a number of simulations starting from perturbed Ince–Gaussian transverse patterns, and the field always converged to the corresponding IGM. Typically, ≈60 round trips were required for the process to converge. As expected, the convergence of the Fox–Li method is a consequence of the fact that IGMs are also eigensolutions of the self-consistency equation for the resonator, namely,

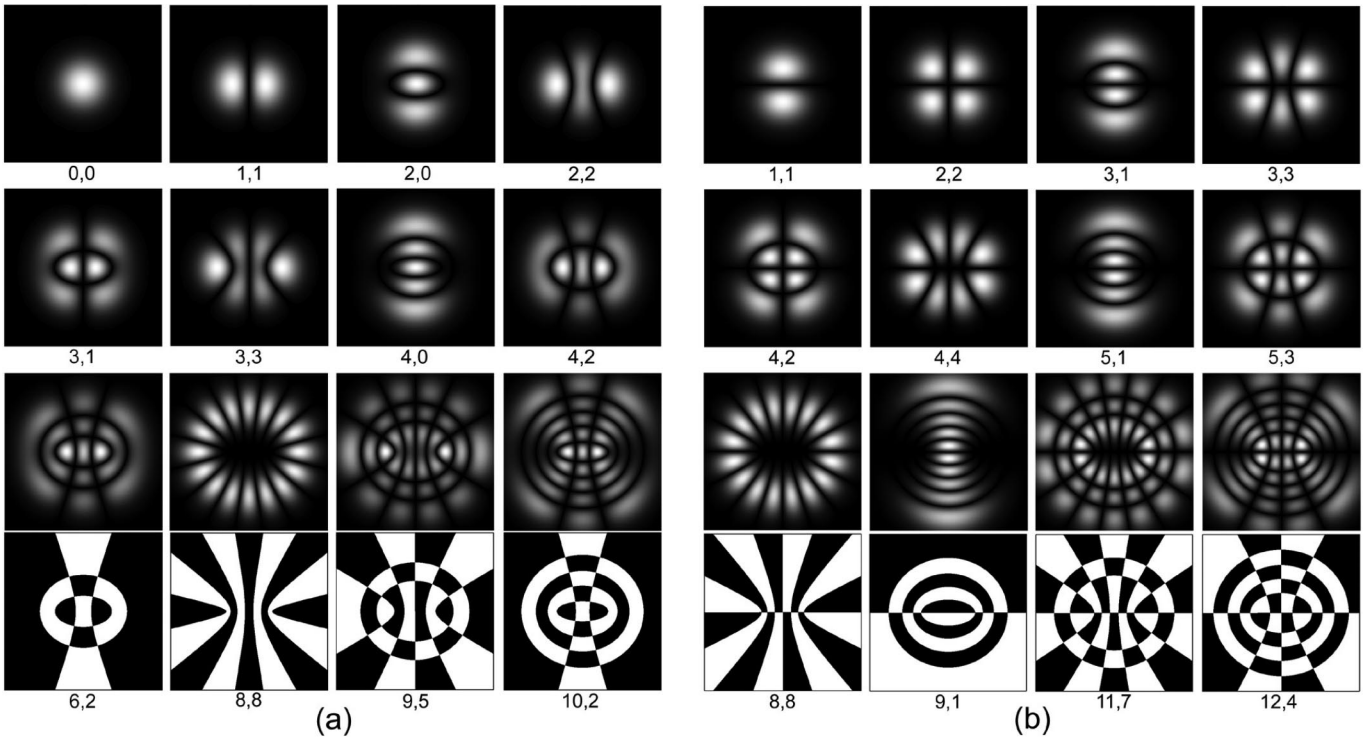

Fig. 1. Transverse field distributions of several low-order (a) even, (b) odd IGMs with $\epsilon = 2$. Plots depicted in the bottom row correspond to the phase structure of the modes displayed in the third row.

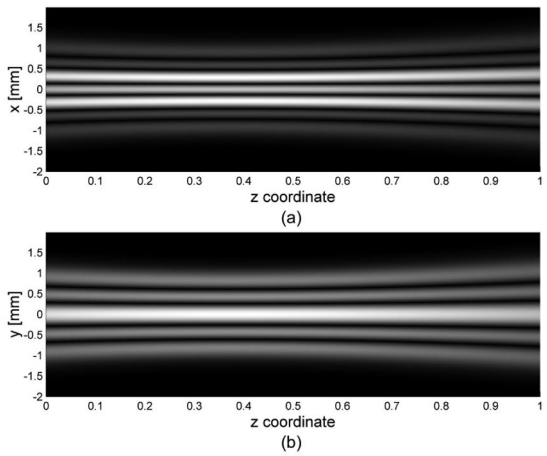

Fig. 2. Passive three-dimensional intracavity field distribution of the mode $\mathrm{IG}^{e}_{6,2}(\xi,\ \eta,\ \epsilon = 2)$ in a two-mirror stable resonator. The waist is located at $z = 0.375$ m.

$$\gamma \mathrm{IG}(\xi_2,\ \eta_2) = \int\int\ K(\xi_2,\ \eta_2,\ \xi_1,\ \eta_1)\mathrm{IG}(\xi_1,\ \eta_1)\mathrm{d}S_1, \tag{12}$$

where γ is the complex eigenvalue, K is the Huygens–Fresnel kernel for the wave propagation through an ABCD paraxial system involving a complete round trip in the cavity from reference plane 1 (coordinates $\xi_1,\ \eta_1$) to reference plane 2 (coordinates $\xi_2,\ \eta_2$), and $\mathrm{d}S_1$ is the differential area element on the plane 1. We finally remark that, as with LGMs and HGMs, the two-dimensional Fourier transform of the transverse distribution of an IGM has the same mathematical form as the original IGM; in other words, IGMs are self-reproducing under the two-dimensional Fourier transform.

4. RELATIONS WITH HERMITE– AND LAGUERRE–GAUSSIAN MODES

We now study the important relations between IGMs on the one hand and LGMs and HGMs on the other. A close examination of these relations reveals the existence of interesting underlying symmetries that these families of modes possess.

We include here explicit expressions of the LGMs and HGMs in order to establish notation and to provide a reference point for appropriate comparisons. The normalized even and odd LGMs with radial number n and azimuthal number l are written as

$$\mathrm{LG}^{e,o}_{n,l}(r,\ \phi,\ z) = \left[\frac{4n!}{(1 + \delta_{0,l})\pi(n + l)!}\right]^{1/2}\frac{1}{w(z)}\begin{pmatrix}\cos l\phi\\ \sin l\phi\end{pmatrix} \times \left[\frac{\sqrt{2}r}{w(z)}\right]^{l} L^{l}_{n}\left(\frac{2r^2}{w(z)^2}\right)\exp\left[\frac{-r^2}{w^2(z)}\right] \times \exp i\left[kz + \frac{kr^2}{2R(z)} - (2n + l + 1)\psi_{\mathrm{GS}}(z)\right], \tag{13}$$

where $L^{l}_{n}(\ \cdot\ )$ are the generalized Laguerre polynomials. The normalized HGMs are given by

$$\mathrm{HG}_{n_x,n_y}(x,\ y,\ z) = \left(\frac{1}{2^{n_x + n_y - 1}\pi n_x! n_y!}\right)^{1/2}\frac{1}{w(z)} \times H_{n_x}\left(\frac{\sqrt{2}x}{w(z)}\right)H_{n_y}\left(\frac{\sqrt{2}y}{w(z)}\right)\exp\left[\frac{-r^2}{w^2(z)}\right] \times \exp i\left[kz + \frac{kr^2}{2R(z)} - (n_x + n_y + 1)\psi_{\mathrm{GS}}(z)\right], \tag{14}$$

where $H_n(\ \cdot\ )$ are the nth order Hermite polynomials.

The transition from an $\mathrm{IG}^{e,o}_{p,m}$ mode to a $\mathrm{LG}^{e,o}_{n,l}$ mode occurs when the elliptic coordinates tend to the circular cylindrical coordinates, i.e., when $f_0 \to 0$. In this limit the indices of both modes are related as follows: $m = l$ and $p = 2n + l$. On the other hand, the transition from an $\mathrm{IG}^{e,o}_{p,m}$ into a HG_{n_x,n_y} occurs when $f_0 \to \infty$; in this case the indices are related as follows: For even IGMs $n_x = m$ and $n_y = p - m$, whereas for odd IGMs $n_x = m - 1$ and $n_y = p - m + 1$. In Fig. 3 we show the transition of some IGMs into their corresponding LGMs and HGMs. It is important to notice in Eq. (7) that in these transitions, p takes the exact value to ensure that the Gouy shift of the IGM is the same Gouy shift of the corresponding LGM or HGM.

Since three types of modes form complete families for expanding an arbitrary paraxial field, one should be able to express one type in terms of either of the others. The HGM⇔LGM expansions have been discussed previously in Refs. 10 and 11.

At any plane z, the IG⇔LG expansions are written as

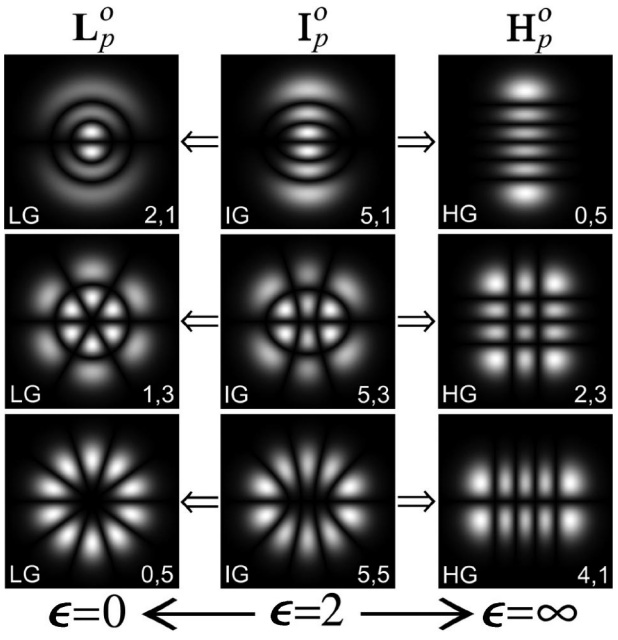

Fig. 3. Transverse shapes of the subsets $\mathbf{L}^o_p$, $\mathbf{I}^o_p$, and $\mathbf{H}^o_p$ for $p = 5$. IGMs correspond to $\epsilon = 2$.

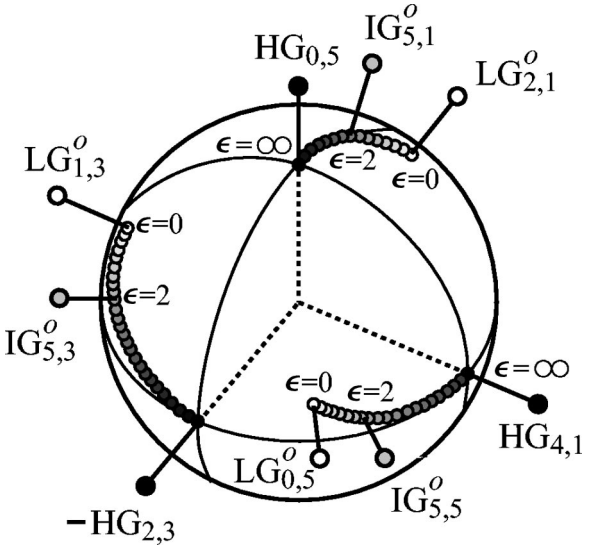

Fig. 4. Graphical representation of the subset $p = 5$ ($N_5 = 3$) in a three-dimensional vector space. The transverse modes are shown in Fig. 3. Each gray circle corresponds to a different value of ϵ. The model $IG^o_{5,3}$ tends to the negative value of $HG^o_{2,3}$ because for some combinations of indices (n_x, n_y), the HGMs of Eq. (14) do not satisfy the standard parity convention about the positive x axis [i.e., if $n = 0,1,2,...$, the even Hermite polynomials $H_{2+4n}(u)$ and the first derivative of the odd Hermite polynomials $H_{3+4n}(u)$ are negative at $u = 0$].

$$\mathrm{LG}^{\sigma}_{n,l}(r,\ \phi) = \sum_m D_m \mathrm{IG}^{\sigma}_{p=2n+l,m}(\xi,\ \eta,\ \epsilon), \quad (15a)$$

$$\mathrm{IG}^{\sigma}_{p,m}(\xi,\ \eta,\ \epsilon) = \sum_{l,n} D_{l,n} \mathrm{LG}^{\sigma}_{n,l}(r,\ \phi), \quad (15b)$$

where $\sigma = \{e, o\}$ is the parity. The coefficients D correspond to the overlap integral between an IGM and a LGM and can be obtained by applying group theory techniques[12]; we have

$$\int\int_{-\infty}^{\infty} \mathrm{LG}^{\sigma}_{n,l}\overline{\mathrm{IG}}^{\sigma'}_{p,m}\mathrm{d}S = \delta_{\sigma'\sigma}\delta_{p,2n+l}(-1)^{n+l+(p+m)/2} \times \sqrt{(1+\delta_{0,l})\Gamma(n+l+1)n!}A^{\sigma}_{(l+\delta_{o,\sigma})/2}(a^m_p), \quad (16)$$

where $A^{\sigma}_{(l+\delta_{o,\sigma})/2}(a^m_p)$ is the $(l+\delta_{o,\sigma})/2$th Fourier coefficient of the C^m_p or S^m_p Ince polynomial (see Appendix A). The coefficients A are scaled out in order to satisfy the normalization condition $\Sigma_j D_j^2 = 1$. Once we know the IG⇔LG relations, the IG⇔HG formulas can be readily obtained by applying the already known LG⇔HG expansions[10] in cascade with the IG⇔LG expansions.

There are some mathematical properties of the expansions among the three families worth discussing here. First, notice that summations (15) are finite. This important result has a simple physical interpretation: To build up a structurally stable beam, the constituent modes must have the same Gouy shift; thus they remain in phase as they propagate. This conclusion applies also for the IG⇔HG and the HG⇔LG relations. In order to satisfy this restriction, the summations of all expansions among the three families must involve a finite number of modes whose indices (n, l) and (n_x, n_y) satisfy the condition $p = 2n + l = n_x + n_y$, for a given p.

It seems appropriate then to split each family of LGMs, IGMs, and HGMs into subsets of degenerate modes that share the same Gouy shift and the same parity about the positive x axis. Let $\mathbf{L}^{\sigma}_p$, $\mathbf{I}^{\sigma}_p$, and $\mathbf{H}^{\sigma}_p$ be the subsets of the (even/odd) LG, IG, or HG modes whose Gouy shift is $\psi_p(z) = (p+1)\psi_{\mathrm{GS}}(z)$, respectively. It is not difficult to see that each subset is composed of

$$N_p = \begin{cases} (p + 2\delta_{\sigma,e})/2, & \text{if } p \text{ is even,} \\ (p+1)/2, & \text{if } p \text{ is odd,} \end{cases} \quad (17)$$

degenerate modes that form a complete subbasis of orthonormal modes under which any Gaussian field with Gouy shift $\psi_p(z)$ can be expanded. Therefore any mode of a given subset (e.g., an $\mathrm{IG}^{\sigma}_{p,m}$ mode) can be constructed as a linear superposition of the N_p modes of the other two subsets (e.g., $\mathrm{LG}^{\sigma}_{n,l}$ or HG_{n_x,n_y} modes).

In Fig. 3 we show a pictorial representation of the three subsets $\mathbf{L}^o_p$, $\mathbf{I}^o_p$, and $\mathbf{H}^o_p$ for $p = 5$. Each subset is composed of $N_p = 3$ orthonormal modes whose common Gouy shift is given by $6\psi_{\mathrm{GS}}(z)$. By evaluating Eq. (16) we can obtain explicit expressions of the IGMs in terms of LGMs and vice versa.

The linear relations between subsets $\mathbf{L}^{\sigma}_p$, $\mathbf{I}^{\sigma}_p$, and $\mathbf{H}^{\sigma}_p$ can be written in a matrix notation as follows:

$$\mathbf{I}^{\sigma}_p = [{}_{LI}\mathbf{T}^{\sigma}_p]\mathbf{L}^{\sigma}_p, \quad (18a)$$

$$\mathbf{H}^{\sigma}_p = [{}_{IH}\mathbf{T}^{\sigma}_p]\mathbf{I}^{\sigma}_p, \quad (18b)$$

$$\mathbf{L}^{\sigma}_p = [{}_{HL}\mathbf{T}^{\sigma}_p]\mathbf{H}^{\sigma}_p, \quad (18c)$$

where the $N_p \times N_p$ transformation matrices $[{}_{AB}\mathbf{T}^{\sigma}_p]$ are real unitary matrices that satisfy $[{}_{AB}\mathbf{T}^{\sigma}_p]^{-1} = [{}_{AB}\mathbf{T}^{\sigma}_p]^T \equiv [{}_{BA}\mathbf{T}^{\sigma}_p]$ and whose columns (and rows) form a basis of N_p orthonormal vectors for the N_pth-dimensional vector space. Since $[{}_{HI}\mathbf{T}^{\sigma}_p] = [{}_{LI}\mathbf{T}^{\sigma}_p]\,[{}_{HL}\mathbf{T}^{\sigma}_p]$, only two matrices in Eqs. (18) are independent. For the subsets depicted in Fig. 3 we have explicitly

$$\begin{pmatrix} \mathrm{IG}^o_{5,1} \\ \mathrm{IG}^o_{5,3} \\ \mathrm{IG}^o_{5,5} \end{pmatrix} = \begin{bmatrix} 0.938 & 0.344 & 0.048 \\ -0.343 & 0.901 & 0.266 \\ 0.048 & -0.266 & 0.963 \end{bmatrix} \begin{pmatrix} \mathrm{LG}^o_{2,1} \\ \mathrm{LG}^o_{1,3} \\ \mathrm{LG}^o_{0,5} \end{pmatrix},$$

$$\begin{pmatrix} \mathrm{IG}^o_{5,1} \\ \mathrm{IG}^o_{5,3} \\ \mathrm{IG}^o_{5,5} \end{pmatrix} = \begin{bmatrix} 0.101 & 0.310 & 0.945 \\ -0.649 & -0.700 & 0.298 \\ 0.755 & -0.643 & 0.130 \end{bmatrix} \begin{pmatrix} \mathrm{HG}_{4,1} \\ \mathrm{HG}_{2,3} \\ \mathrm{HG}_{0,5} \end{pmatrix}.$$

Notice that while the elements of $[{}_{HL}\mathbf{T}^{\sigma}_p]$ depend exclusively on the indices (n, l) and (n_x, n_y), the elements of $[{}_{LI}\mathbf{T}^{\sigma}_p]$ and $[{}_{IH}\mathbf{T}^{\sigma}_p]$ depend also on the continuous ellipticity parameter ϵ. In Fig. 4 we show a graphical representation of the subset $p = 5$ ($N_p = 3$) in a three-

Table 1. The Four "Fundamental" Modes

Shape	Parity	HG_{n_x,n_y}	$\mathrm{LG}^{\sigma}_{n,l}$	$\mathrm{IG}^{\sigma}_{p,m}$
○	$\sigma = e$	0,0	0,0	0,0
∞	$\sigma = e$	1,0	0,1	1,1
8	$\sigma = o$	0,1	0,1	1,1
⊕	$\sigma = 0$	1,1	0,2	2,2

dimensional vector space. The subsets $\mathbf{H}_5^o$, $\mathbf{L}_5^o$, and $\mathbf{I}_5^o$ are associated with three orthonormal triads with common origin, the unit vectors of a "fixed" Cartesian triad are associated with the elements of $\mathbf{H}_5^o$, the unit vectors of a "rotated" triad are associated with the elements of $\mathbf{L}_5^o$, and the unit vectors of a "movable" triad are associated with the elements of $\mathbf{I}_5^o$. As expected, the matrices $[{}_{HL}\mathbf{T}_5^o]$ and $[{}_{HI}\mathbf{T}_5^o]$ are the rotation matrices of the Laguerre and Ince triads. The continuous transition of $\mathbf{I}_5^o$ from $\mathbf{L}_5^o$ to $\mathbf{H}_5^o$ can be parametrized by the ellipticity ϵ of the IGMs; see Fig. 4.

A very remarkable consequence of the relations among IGMs, LGMs, and HGMs is the existence of four special modes that (given w_0) have exactly the same transverse distribution, independently of the basis used to describe them. In Table 1 we include the pairs of indices of the four "fundamental" modes for each of the three families of Gaussian beams. The symbols in the leftmost column are graphical representations of the mode shapes. The transverse patterns are already shown in Fig. 1. The $e(o)$ in the second column refers to the even (odd) parity of the mode about the positive x axis. The existence of these fundamental modes can be explained by noting in Eq. (17) that for the given combinations of indices, only one constituent mode is needed to build up the other. The existence of these invariant modes is particularly interesting because it reveals the underlying symmetries and connections between the exact families of solutions of the PWE.

5. HELICAL INCE–GAUSSIAN MODES

LGMs with azimuthal angular dependence $\exp(\pm il\varphi)$ have a phase that rotates circularly about the propagation axis.[3,13] In a similar way, from the stationary mode solutions described by Eq. (7) it is possible to construct helical IGMs (HIGM) of the form

$$\mathrm{HIG}_{p,m}^{\pm} = \mathrm{IG}_{p,m}^{e}(\xi,\ \eta,\ \epsilon) \pm i\,\mathrm{IG}_{p,m}^{o}(\xi,\ \eta,\ \epsilon), \quad (19)$$

but whose phase now rotates elliptically around a line defined by $(|x| \leqslant f,\ 0,\ z)$. The sign in Eq. (19) defines the rotating direction. Equation (19) is valid for $m > 0$ because $\mathrm{IG}_{p,m}^{o}$ is not defined for $m = 0$. In Fig. 5 we show the transverse magnitudes and phases of the stationary modes $\mathrm{IG}_{10,6}^{e,o}$ $(\xi,\ \eta,\ \epsilon = 1)$ and the corresponding HIGM at the waist plane. For this combination of indices, the pattern consists of three well-defined elliptic confocal rings with a dark elliptic spot on axis; thus it seems appropriate to refer to this kind of hollow beam as "elliptic donut modes." For the general case, the number of rings is given by the relation $1 + (p - m)/2$; thus, a single elliptic donut can be generated with modes for which $p = m$.

The vortices of a scalar field are found where the real and imaginary components of this field are zero. For a mode $\mathrm{HIG}_{p,m}^{\pm}$ the principal branch points of elliptic vortices occur along the interfocal line $(\xi = 0)$ at points $x_j = f\cos\eta_j$, where $j = 1,\ldots,m$, and η_j are the zeros of the Ince polynomial $C_p^m(\eta,\ \epsilon)$ in the interval $(0,\ \pi)$. Whereas for $m = 1$ the phase rotates about the z axis, for higher-order modes it rotates about a line in the x axis defined by points x_1 and x_m, the width of which is always smaller than $2f$. The phase then is formed by m in-line vortices, each with unitary topological charge such that the total charge is m.

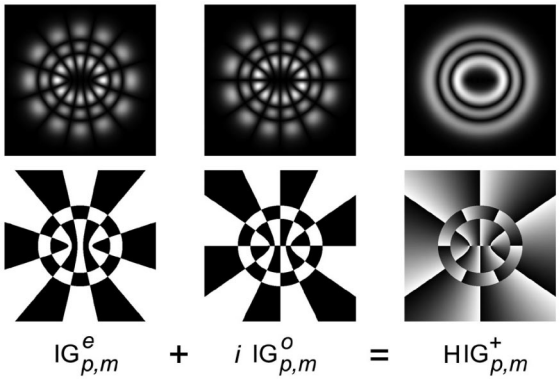

Fig. 5. Transverse amplitudes and phases of stationary modes $\mathrm{IG}_{10,6}^{o}(\xi,\ \eta,\ \epsilon = 1)$ and the corresponding HIGM at the waist plane. Note that the phase rotates around the line joining the foci of the ellipses. Contiguous rings have a π phase jump.

We remark that HIGMs exhibit rotating and vortical features similar to those of the so-called high-order Mathieu beams[14–16] that are exact propagating-invariant solutions of the Helmholtz equation in elliptic coordinates. The HIGMs presented here can be applied to construct elliptic optical tweezers[17] and atom traps as well to study the transfer of angular momentum to microparticles or atoms.[18]

6. CONCLUSION

We have demonstrated in this work that an alternative but equally valid complete family of resonating modes in stable resonators can be written in elliptic coordinates rather than in Cartesian or circular cylindrical coordinates. The IGMs are exact and orthogonal solutions to the PWE and constitute the exact and continuous transition modes between LGMs and HGMs. The known methods of propagating Hermite and Laguerre beams through paraxial optical systems (e.g., bilinear transformation of the parameter q, Huygens–Fresnel integral diffraction, and angular spectrum of plane waves) can also be applied to propagate IGMs. IGMs exhibit an inherent elliptical structure whose shape remains invariant (ignoring a scaling factor) as they propagate.

The transformation matrices relating the IGMs to the LGMs and HGMs have been derived and discussed. Besides their theoretical importance, we think that these relations are useful in problems of mixed symmetry. Possible examples include the diffraction of LGMs by elliptical apertures, or the expansion of an IGM when it has to be integrated over rectangular coordinates, or in measurements of mechanical torque induced by transitions between LGMs and HGMs.[3]

It is convenient to mention that the results discussed in this work within the context of optics are related to other areas of physics. For instance, the IGMs also constitute a family of solutions of the two-dimensional time-dependent Schrödinger equation for a free particle. On the other hand, IGMs at the waist plane correspond to the eigenstates of the two-dimensional quantum harmonic oscillator.

APPENDIX A: INCE POLYNOMIALS

Ince polynomials are very interesting and do not seem to have attracted the attention they deserve; little, indeed, is known about them. In this appendix we include the basic theory and properties of Ince polynomials; we refer the interested reader to Arscott[6,7] for details.

Ince Eq. (5) is a periodic linear second-order differential equation that has two families of independent solutions, namely, the even $C_p^m(\eta,\epsilon)$ and odd $S_p^m(\eta,\epsilon)$ Ince polynomials of order p and degree m. Physical considerations are such that Ince polynomials are periodic with period 2π. The values of a in Eq. (5) that satisfy this condition are the eigenvalues of the equation; for C_p^m the eigenvalues are denoted as $a_p^m(\epsilon)$, and for S_p^m they are denoted as $b_p^m(\epsilon)$. Given p and $\epsilon > 0$, the eigenvalues form a finite set of real values that have the property $a_p^0 < b_p^1 < a_p^1 < b_p^2 \cdots < a_p^p < b_p^p$. Each function C_p^m and S_p^m is associated with an eigenvalue a_p^m or b_p^m that in turn depends on ϵ.

C_p^m and S_p^m are periodic and can be expanded in finite trigonometric series. The corresponding expansions fall into four classes, according to their symmetry or antisymmetry, about $\eta = 0$ and $\eta = \pi/2$, namely,

$$C_{2n}^{2k}(\eta,\epsilon) = \sum_{r=0}^{n} A_r \cos 2r\eta, \qquad k = 0,..,n, \tag{A1a}$$

$$C_{2n+1}^{2k+1}(\eta,\epsilon) = \sum_{r=0}^{n} A_r \cos(2r+1)\eta, \qquad k = 0,..,n, \tag{A1b}$$

$$S_{2n}^{2k}(\eta,\epsilon) = \sum_{r=1}^{n} B_r \sin 2r\eta, \qquad k = 1,..,n, \tag{A1c}$$

$$S_{2n+1}^{2k+1}(\eta,\epsilon) = \sum_{r=0}^{n} B_r \sin(2r+1)\eta, \qquad k = 0,..,n. \tag{A1d}$$

Three-term recurrence relations between the coefficients can be derived by substituting series (A1) into Eq. (5).

For $C_{2n}^{2k}(\eta,\epsilon)$, $p = 2n$:

$$(p/2+1)\epsilon A_1 = aA_0,$$

$$(p/2+2)\epsilon A_2 = -p\epsilon A_0 - (4-a)A_1,$$

$$(p/2+r+2)\epsilon A_{r+2} = [a - 4(r+1)^2]A_{r+1} + \left(r - \frac{p}{2}\right)\epsilon A_r,$$

For $S_{2n}^{2k}(\eta,\epsilon)$, $p = 2n$;

$$(p/2+2)\epsilon B_2 = (a-4)B_1,$$

$$(p/2+r+2)\epsilon B_{r+2} = [a - 4(r+1)^2]B_{r+1} + \left(r - \frac{p}{2}\right)\epsilon B_r,$$

For $C_{2n+1}^{2k+1}(\eta,\epsilon)$, $p = 2n+1$:

$$\frac{\epsilon}{2}(p+3)A_1 = \left[a - \frac{\epsilon}{2}(p+1) - 1\right]A_0,$$

$$\frac{\epsilon}{2}(p+2r+3)A_{r+1} = [a - (2r+1)^2]A_r + \frac{\epsilon}{2}(2r-p-1)A_{r-1},$$

For $S_{2n+1}^{2k+1}(\eta,\epsilon)$, $p = 2n+1$;

$$\frac{\epsilon}{2}(p+3)B_1 = \left[a + \frac{\epsilon}{2}(p+1) - 1\right]B_0,$$

$$\frac{\epsilon}{2}(p+2r+3)B_{r+1} = [a - (2r+1)^2]B_r + \frac{\epsilon}{2}(2r-p-1)B_{r-1};$$

$r = 1, 2,...,n$ for the four cases. The usual approach for finding the eigenvalues and coefficients is based on constructing finite tridiagonal matrices from the recurrence relations. The eigenvalues and eigenvectors of these matrices are the eigenvalues a_p^m, b_p^m of the Ince equation and the coefficients A_r, B_r of the trigonometric series.[6]

To summarize, Ince polynomials are denoted as $C_p^m(\eta,\epsilon)$ and $S_p^m(\eta,\epsilon)$, where $0 \leqslant m \leqslant p$ for even functions; $1 \leqslant m \leqslant p$ for odd functions; the indices (p, m) have the same parity, i.e., $(-1)^{p-m} = 1$; and ϵ is the ellipticity parameter.[6]

The behavior of Ince polynomials is fairly complicated, particularly because we need to understand the dependence of the functions on the variable η and the parameters (ϵ, p, m). The parity, periodicity, and normalization of the Ince polynomials are exactly the same as for their trigonometric counterparts. That is, $C_p^m(\eta,\epsilon)$ is even and $S_p^m(\eta,\epsilon)$ is odd, and they have period π when m

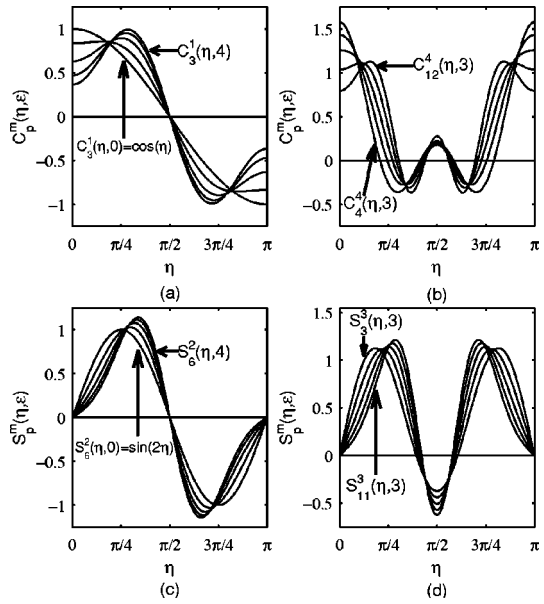

Fig. 6. Plots of Ince polynomials (a) $C_3^1(\eta,\epsilon)$, $\epsilon \in \{0, 1, 2, 3, 4\}$; (b) $C_p^4(\eta, 3)$, $p \in \{4, 6, 8, 10, 12\}$; (c) $S_6^2(\eta,\epsilon)$, $\epsilon \in \{0, 1, 2, 3, 4\}$; (d) $S_p^3(\eta, 3)$, $p \in \{3, 5, 7, 9, 11\}$.

is even or period 2π when m is odd. Ince polynomials have m zeros in $0 \leqslant \eta < \pi$ for all values of ϵ, but they tend to cluster about $\eta = \pi/2$ as ϵ increases. As $\epsilon \to 0$, $C_p^m(\eta, \epsilon) \to \cos m\eta$ and $S_p^m(\eta, \epsilon) \to \sin m\eta$. In Fig. 6 we plot the functions $C_p^m(\eta, \epsilon)$ and $S_p^m(\eta, \epsilon)$ for several values of the parameters p, m, and ϵ in the range $0 \leqslant \eta \leqslant \pi$. Ince polynomials satisfy the orthogonality relation, which is

$$\int_{-\pi}^{\pi} \exp\left(-\frac{\epsilon}{2}\cos 2\eta\right) C_p^m(\eta, \epsilon) C_p^{m'}(\eta, \epsilon) \mathrm{d}\eta = 0, \quad m \neq m'. \tag{A2}$$

Radial Eq. (4) is obtained from Eq. (5) by setting the change of variable $\eta = i\xi$; then applying this change of variable to Eq. (A1), we obtain the following expansions for the radial Ince polynomials:

$$C_{2n}^{2k}(i\xi, \epsilon) = \sum_{r=0}^{n} A_r \cosh 2r\eta, \tag{A3a}$$

$$C_{2n+1}^{2k+1}(i\xi, \epsilon) = \sum_{r=0}^{n} A_r \cosh(2r+1)\eta, \tag{A3b}$$

$$S_{2n}^{2k}(i\xi, \epsilon) = \sum_{r=1}^{n} B_r \sinh 2r\eta, \tag{A3c}$$

$$S_{2n+1}^{2k+1}(i\xi, \epsilon) = \sum_{r=0}^{n} B_r \sinh(2r+1)\eta, \tag{A3d}$$

where the coefficients A and B are the same as in Eq. (A1).

ACKNOWLEDGMENTS

The authors thank Kurt Bernardo Wolf for helpful discussions. This research was partially supported by Consejo Nacional de Ciencia y Tecnología of México and by the Tecnológico de Monterrey Research Chair in Optics under grant CAT-007.

Corresponding author Julio C. Gutiérrez-Vega can be reached by e-mail at juliocesar@itesm.mx. Miguel A. Bandres is also with the Department of Physics and Astronomy, State University of New York at Stony Brook, Stony Brook, New York 11794-3800, and can be reached by e-mail at mbandres@grad.physics.sunysb.edu.

REFERENCES

1. A. E. Siegman, *Lasers* (University Science, Mill Valley, Calif., 1986).
2. H. Kogelnik and T. Li, "Laser beams and resonators," Proc. IEEE **54**, 1312–1329 (1966).
3. L. Allen, M. W. Beijersbergen, R. J. C. Spreeuw, and J. P. Woerdman, "Orbital angular momentum of light and the transformation of Laguerre-Gaussian laser modes," Phys. Rev. A **96**, 8185–8194 (1992).
4. G. Nienhuis and L. Allen, "Paraxial wave optics and harmonic oscillators," Phys. Rev. A **48**, 656–665 (1993).
5. E. G. Ince, "A linear differential equation with periodic coefficients," Proc. London Math. Soc. **23**, 56–74 (1923).
6. F. M. Arscott, *Periodic Differential Equations* (Pergamon, Oxford, UK, 1964).
7. F. M. Arscott, "The Whittaker-Hill equation and the wave equation in paraboloidal coordinates," Proc. R. Soc. Edinburgh Sect. A **67**, 265–276 (1967).
8. M. Abramowitz and I. A. Stegun, *Handbook of Mathematical Functions* (Dover, New York, 1964), Chap. 19.
9. A. G. Fox and T. Li, "Resonant modes in maser interferometer," Bell Syst. Tech. J. **40**, 453–488 (1961).
10. I. Kimel and L. R. Elías, "Relations between Hermite and Laguerre Gaussian modes," IEEE J. Quantum Electron. **29**, 2562–2567 (1993).
11. A. T. O'Neil and J. Courtial, "Mode transformations in terms of the constituent Hermite–Gaussian or Laguerre–Gaussian modes and the variable-phase converter" Opt. Commun. **181**, 35–45 (2000).
12. C. P. Boyer, E. G. Kalnins, and W. Miller, Jr., "Lie theory and separation of variables. 7. The harmonic oscillator in ellipic coordinates and the Ince polynomials," J. Math. Phys. **16**, 512–523 (1975).
13. L. Allen, M. J. Padgett, and M. Babiker, "The orbital momentum of light," Prog. Opt. **39**, 291–371 (1999).
14. J. C. Gutiérrez-Vega, M. D. Iturbe-Castillo, and S. Chávez-Cerda, "Alternative formulation for invariant optical fields: Mathieu beams," Opt. Lett. **25**, 1493–1495 (2000).
15. J. C. Gutiérrez-Vega, M. D. Iturbe-Castillo, G. A. Ramírez, E. Tepichín, R. M. Rodríguez-Dagnino, S. Chávez-Cerda, and G. H. C. New, "Experimental demonstration of optical Mathieu beams," Opt. Commun. **195**, 35–40 (2001).
16. S. Chávez-Cerda, J. C. Gutiérrez-Vega, and G. H. C. New, "Elliptic vortices of electromagnetic wave fields," Opt. Lett. **26**, 1803–1805 (2001).
17. J. Arlt and M. J. Padgett, "Generation of a beam with a dark focus surrounded by regions of higher intensity," Opt. Lett. **25**, 191–193 (2000).
18. K. T. Gahagan and G. A. Swartzlander, Jr., "Optical vortex trapping of particles," Opt. Lett. **21**, 827–829 (1997).